NeuroImage 42 (2008) 945–955

Contents lists available at ScienceDirect

NeuroImage

journal homepage: www.elsevier.com/locate/ynimg

Selective activation of the superior frontal gyrus in task-switching: An event-related fNIRS study

Simone Cutini [a,*], Pietro Scatturin [b], Enrica Menon [b], Patrizia Silvia Bisiacchi [a], Luciano Gamberini [a], Marco Zorzi [a], Roberto Dell'Acqua [b]

[a] Department of General Psychology, Padova, Italy
[b] Department of Developmental Psychology and Socialization, Padova, Italy

ARTICLE INFO

Article history:
Received 18 March 2008
Revised 5 May 2008
Accepted 6 May 2008
Available online 20 May 2008

ABSTRACT

In the task-switching paradigm, reaction time is longer and accuracy is worse in switch trials relative to repetition trials. This so-called *switch cost* has been ascribed to the engagement of control processes required to alternate between distinct stimulus–response mapping rules. Neuroimaging studies have reported an enhanced activation of the human lateral prefrontal cortex and the superior frontal gyrus during the task-switching paradigm. Whether neural activation in these regions is dissociable and associated with separable cognitive components of task switching has been a matter of recent debate. We used multi-channel near-infrared spectroscopy (fNIRS) to measure brain cortical activity in a task-switching paradigm designed to avoid task differences, order predictability, and frequency effects. The results showed a generalized bilateral activation of the lateral prefrontal cortex and the superior frontal gyrus in both switch trials and repetition trials. To isolate the activity selectively associated with the task-switch, the overall activity recorded during repetition trials was subtracted from the activity recorded during switch trials. Following subtraction, the remaining activity was entirely confined to the left portion of the superior frontal gyrus. The present results suggest that factors associated with load and maintenance of distinct stimulus–response mapping rules in working memory are likely contributors to the activation of the lateral prefrontal cortex, whereas only activity in the left superior frontal gyrus can be linked unequivocally to switching between distinct cognitive tasks.

Introduction

The popularity of the task-switching paradigm as a tool for exploring the role of control in the human cognitive architecture has increased enormously since its original introduction in the psychological literature (Jersild, 1927; see Monsell, 2003, for a review). In a typical task-switching experiment, subjects are instructed to repeat the same task over a variable number of trials, and switch to a different task at some point during the trial sequence. Each task often involves a speeded response, and a reaction time (RT) is usually recorded. The finding of interest is that the mean RT in switch trials is longer than the mean RT in repetition trials. This RT difference has been labeled *switch cost* (Rogers and Monsell, 1995). Although different under a number of aspects, models of the task-switching share a set of core assumptions concerning the functional source of switch costs. One such assumption is that switch costs reflect the time taken to abandon a particular stimulus–response mapping rule demanded for the execution of one task and load a different stimulus–response mapping rule demanded for the execution of a different task. The models proposed differ, however, with regard to the interplay between the functional mechanisms subtended in the execution of the different tasks. Briefly, while some have argued that the switch costs result from the time taken to implement a relevant stimulus–response mapping rule (or task-set), or, more in general, alternate between the relevant perceptual and motor parameters for the different tasks (Meiran, 1996; Meiran et al., 2000; Rogers and Monsell, 1995; Rubinstein et al., 2001), others investigators have instead emphasized the role of cross-task interference as a major determinant of switch costs (Allport et al., 1994; Waszak et al., 2003; Yeung and Monsell, 2003).

There have been several attempts to localize in the human brain the neural substrate of the set of complex functional routines subtended in task-switching. Most of the neuroanatomical evidence collected so far converge to suggest that the lateral prefrontal cortex (latPFC; e.g., Dove et al., 2000; Dreher

* Corresponding author. Department of General Psychology, Via Venezia 8, 35131 Padova, Italy. Fax: +39 049 827 6600.
E-mail address: simone.cutini@unipd.it (S. Cutini).

1053-8119/$ – see front matter © 2008 Elsevier Inc. All rights reserved.
doi:10.1016/j.neuroimage.2008.05.013

and Berman, 2002; Sohn et al., 2000), and regions in the superior frontal gyrus (sFG; Crone et al., 2006; Rushworth et al., 2002, Slagter et al., 2006), such as the pre-supplementary and supplementary motor areas (pre-SMA and SMA; Dove et al., 2000; Crone et al., 2006; Rushworth et al., 2002), play a prominent role in task-switching, even though the specific functional operations of each of these brain areas in this experimental context is still a matter of debate.

Neuropsychological studies have reported that patients with lesions to the latPFC tend to show an exacerbated task-switch cost relative to controls (Mecklinger et al., 1999; Rogers et al., 1998; but see Dell'Acqua et al., 2003, 2006a,b). Furthermore, neuroimaging studies have found an increased activation of the latPFC in switch trials compared with repetition trials (Dove et al., 2000; Dreher and Grafman, 2003). In contrast with these studies, Stuss et al. (2000) found that patients affected by lesions to the medial sFG manifest a particularly pronounced increase in the rate of incorrect perseverations in the Wisconsin Card Sorting Test. This symptom was hypothesized to arise from the selective inability of these patients to switch between different task rules. More relevant vis-à-vis task-switching, Rushworth et al. (2002), in a study combining fMRI imaging and transcranic magnetic stimulation (TMS) to monitor and modulate the cortical activity during a task-switching paradigm, found a larger blood-oxygen level-dependent (BOLD) response in the sFG/pre-SMA region in switch trials than in repetition trials. Interestingly, TMS inhibitory pulses over sFG/pre-SMA region prolonged RTs in switch trials, but not RTs in repetition trials.

Analogous findings have been described by Crone et al. (2006) in an fMRI study showing a sizable increase in sFG activity in switch trials relative to repetition trials that was associated with close-to-nil variations of activity in the latPFC across these two types of trials. Crone et al. (2006) proposed a unifying account of role of the latPFC and the sFG in task-switching. In these authors' view, the latPFC would be primarily involved in the maintenance and coordination of the different stimulus–response mapping rules in working memory (see also Arbuthnott and Frank, 2000; Baddeley et al., 1998; Mayr and Keele, 2000). In this vein, several factors may be hypothesized to modulate activity in the latPFC in the task-switching paradigm, such as the load imposed by stimulus–response mappings rules when these rules differ between the two tasks subjects have to alternate, or the level of preparation for a specific task when one task must be carried out more frequently than the other task in the task-switching paradigm (see the Discussion for details). On the other hand, the sFG would be more directly related to reconfiguring the cognitive parameters demanded by the execution of a specific task upon detection of a stimulus feature associated with a task-switch, the process usually referred to as task-set reconfiguration (e.g., Monsell, 2003). According to the account proposed by Crone et al. (2006), both latPFC and sFG would be engaged while carrying out a task-switching paradigm, but only the sFG would be determinant for switching between tasks per se.

To test the hypothesis put forth by Crone et al. (2006), we used a task-switching design specifically devised to keep working memory load constant across the tasks chosen in the present investigation. Fig. 1 illustrates a schematic example of a trial sequence. Punctuate stimuli, displayed one at the time at the center of the screen, were used, each of which was associated with a two-alternative speed choice response. The color of the stimuli served as a cue to indicate which particular stimulus–response mapping rule subjects had to adopt to provide a correct response to a given stimulus, and the pair of possible (manual) responses between the two tasks implemented in the present design was kept constant. The frequency with which subjects had to execute each task was

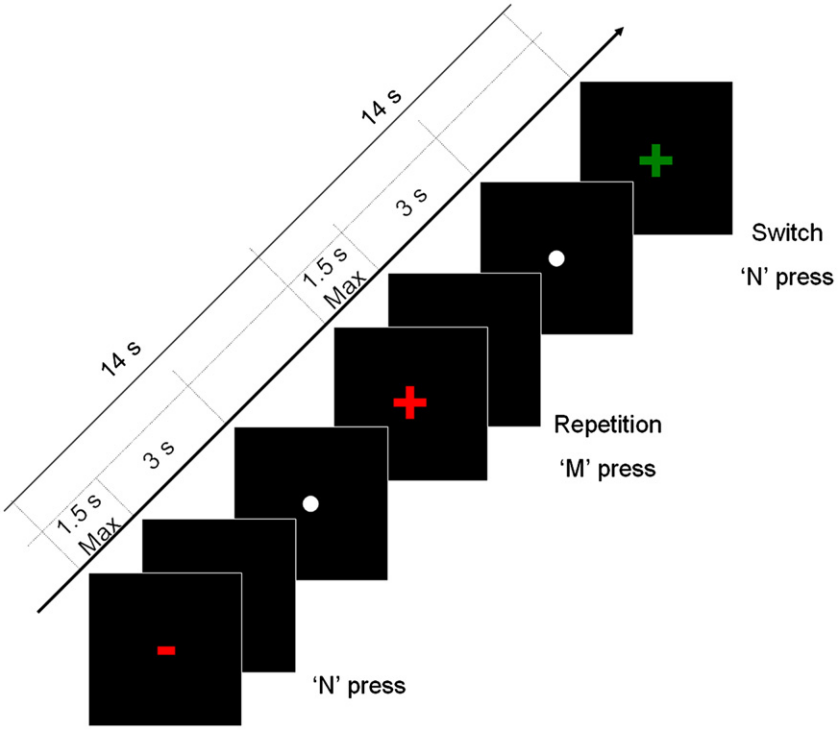

Fig. 1. A schematic illustration of the sequence of events in the present paradigm.

the same, and the tasks order was unpredictable, so as to reduce to a minimum the possibility to anticipate and/or prepare for a task-switch. To monitor the cortical brain activity during the experiment, we employed functional near-infrared spectroscopy (fNIRS), a non-invasive neuroimaging technique that measures changes in oxyhemoglobin (HbO), deoxyhemoglobin (HbR), and total-hemoglobin (HbT) concentrations (Hoshi et al., 2001; Strangman et al., 2002; Villringer and Chance, 1997). At present, the fNIRS technique has been employed in investigations on the sensorimotor apparatus (Miyai et al., 2001; Shimada et al., 2004; Tanosaki et al., 2001), visual perception (Schroeter et al., 2004; Taga et al., 2003), language (Sato et al., 1999), and executive functions (Hoshi et al., 2003; Schroeter et al., 2002). Despite the relatively low spatial resolution and restricted coverage of brain areas with respect to different imaging techniques (e.g., fMRI), the use of fNIRS can be associated with several advantages. For instance, fNIRS imposes negligible physical/motor constraints on the subjects, such that movements can be natural, or nearly so. Furthermore, the NIRS technique is characterized by levels of temporal resolution and signal-to-noise ratio that make it particularly appropriate in the context of event-related task designs.

To isolate the neural substrate of task-switching, and possibly dissociate the different functions implemented in the latPFC and the sFG, we measured the overall cortical activation in repetition trials and in switch trials, and subtracted one estimate from the other. Based on the assumption that working memory load and preparation were constant between the two tasks of the present design, we predicted that a generalized activation of the latPFC and of sFG would be observed in both repetition and switch trials, but that only activity in the sFG would be observed following the subtraction of the overall level of activity observed in repetition trials from the activity observed in switch trials.

Materials and methods

Subjects

Ten right-handed students at the University of Padova (six female; mean age 27.6, range 24–33) participated in the experiment after providing informed consent. All subjects had normal or corrected to-normal vision, and normal color vision. No participant reported a prior history of neurological or psychiatric disorders, and none was under medication at the time of testing.

Stimuli and procedure

During the experiment, each subject was seated in a comfortable chair placed inside a sound-attenuated and dimly lit room, and instructed to rest the index and middle fingers of the right hand on the 'M' and 'N' keys of the computer keyboard throughout the entire experiment. As shown in Fig. 1, each trial began with the presentation of a '+' or '−' on a black screen. These stimuli could be displayed in red or green color. Upon the presentation of a green stimulus, subjects had to press the 'N' in response to a '+', or the 'M' key in response to a '−.' Upon the presentation of a red stimulus, subjects had to use the reversed mapping, pressing 'M' in response to a '+', and 'N' in response to a '−.' Each stimulus was presented for a maximum of 1.5 s, and replaced with a blank screen upon detection of a response. Following a response, 3 s elapsed before the presentation of a central fixation point (a small white dot) for the next trial. After a 5 min of practice, subjects performed a sequence of 120 experimental trials. Stimulus type (+ or −) and color (red or green) were varied orthogonally, in order to include in the sequence an equal number of repetition trials (i.e., 60 trials in which the responses were repeated in accordance with a given stimulus–response mapping rule) and switch trials (60 trials in which a given stimulus–response mapping rule had to be reversed), with the constraint that no more than 6 consecutive repetition/switch trials could occur successively. The order of repetition trials and switch trials was randomized, and was different for each subject.

fNIRS data acquisition

The recording optical unit was a multi-channel frequency-domain NIR spectrometer (ISS Imagent™, Champaign, Illinois), equipped with 32 laser diodes (16 emitting light at 690 nm, and 16 at 830 nm) modulated at 110.0 MHz. The diode-emitted light was conveyed to the subject's head by multimode core glass optical fibers (heretofore, sources; OFS Furukawa LOWOH series fibers, 0.37 of numerical aperture) with a length of 250 cm and a core diameter of 400 μm. Light that scattered through the brain tissue was carried by detector optical fiber bundles (diameter 3 mm) to 4 photo-multiplier tubes (PMTs; R928 Hamamatsu Photonics). The PMTs were modulated at 110.005 MHz, generating a 5.0 KHz heterodyning (cross-correlation) frequency. To separate the light as a function of source location, the sources time-shared the 4 parallel PMTs via an electronic multiplexing device. Only two sources (one per hemisphere) were synchronously (t=4 ms) active (i.e., emitting light), such that the resulting sampling frequency was f=15.0625 Hz, due to the 64 ms sampling period required to cycle through the 16 multiplexed channels. To stabilize the optical signal, a dual-period averaging was performed, resulting in a final sampling period of 128 ms ($f=10^3/128=7.8125$ Hz).

Following detection and consequent amplification by the PMTs, the optical signal was converted into alternating current (AC), direct current (DC), and phase (Φ) signal for each source-detector channel, considering separately each light wavelength. These values were then converted into estimates of absorption coefficient variations ($\Delta\mu\alpha$) using the differential-pathlength factor (DPF; Cope and Delpy, 1988) method. Estimates resulting from the application of the DPF method (sensitive to age differences; see Schroeter et al., 2003, 2004) were age-corrected using the equations described by Duncan et al. (1996):

$$\mathrm{DPF}^{\mathrm{Hb0}} = 5.13 + 0.07*\left(\mathrm{age}^{0.81}\right) \quad (1)$$

$$\mathrm{DPF}^{\mathrm{HbR}} = 4.67 + 0.062*\left(\mathrm{age}^{0.877}\right) \quad (2)$$

Temporal variations (Δ) in the cerebral oxy-hemoglobin (ΔHbO) and deoxy-hemoglobin (ΔHbR) concentrations were calculated based on the values of $\Delta\mu\alpha$ at the two wavelengths (Franceschini et al., 2000; Sevick et al., 1991).

Probe placement procedure

A single-distance probe arrangement, as that described by Franceschini et al. (2000), was adopted in the present context. This arrangement allowed us to maximize the number of HbO–HbR measurement sites. Each source location (illustrated in

Fig. 2a) comprised two source optical fibers, one for each wavelength. The distance between each source/detector pair (heretofore, channel) was L=30.0 mm, in order to equate the channels for optical penetration depth (25 mm circa) into the cortical tissue (Franceschini et al., 2000). Sources and detectors were held in place on the scalp using a custom-made head-mount system provided with velcro straps. The head-mount system was composed of a black rubber foil (external surface) and soft neoprene foam (internal surface, facing the scalp), in order to minimize the potential interference from the environmental light.

The probe placement was performed in accordance with the international 10/20 system (emitter caudal and detector cranial; Okamoto et al., 2004). In Figs. 2b and c, the positions of the sources are odd numbered from 1 to 9, and the detectors are labeled with A, B, C and D. In Fig. 2c, each channel is indicated by the letter of the corresponding detector and by the number of the linked source. The channel-midpoint coincided with the bisection of the source-detector segment. As illustrated in Fig. 2c, the midpoints of the channels A3, A9, and B5 over the left hemisphere were positioned as close as possible to the F3, F1, and C1 sites, respectively. A symmetrical positioning system was used over the right hemisphere for the channels C9, C3 and D5, using the F4, F2 and C2 sites, respectively, as reference points. This spatial arrangement generated a triple spatial bind that allowed us to equate source-detectors alignment and positioning across subjects.

To check for the correct position of the probes over both hemispheres, we performed a cranio-cerebral structural correlation between the positions of sources, detectors and midpoints. A spatial conversion from 10/20 positioning system to Talairach coordinates was carried out using the Talairach-to-10/20 Converter (T2T-converter; http://wwwneuro03.uni-muenster.de/ger/t2tconv/), as an alternative to the probabilistic conversion system proposed by Okamoto et al. (2004), which was optimized for non-Caucasian subjects. Talairach coordinates were subsequently converted in Montreal Neurological Institute (MNI) coordinates through non-linear transformation (Brett et al., 2001). Furthermore, source and detector positions were remapped onto a reference brain. The three-dimensional brain images illustrated in Figs. 2b and c were generated by extracting brain and scalp from the MRI template MNI-ICBM152, and remapping the stereotaxic points onto the reference brain using appropriate software (TCL; Visualization Toolkit, VTK, Kitware Inc.). Fig. 2b shows a reference brain with an indication of the four detectors (green dots) as positioned on the scalp and their projection on the brain according to a minimum-distance criterion on the scalp. Fig. 2c shows the approximate positions of the entire set of sources (red dots) and detectors (green dots) over the transparent scalp surface of the reference brain. As an additional check, the mean source-detector distance was estimated assuming as constant the cortex-scalp distance at all monitored locations (e.g., Ayaz et al., 2006), resulting in a mean source-detector distance of 30.6± 4.6 mm (standard deviation, SD). To note, the degree of precision achieved with this procedure was comparable with that obtained using more rigorous criteria (Okamoto et al., 2004, Okamoto and Dan, 2005; Singh et al., 2005), and yielded a worst-case average error in the conversion process of about 1 cm, which was substantially smaller than the 2.5–3 cm resolution that our particular arrangement of fNIRS channels allowed us to achieve. Fig. 2c shows that both sFG and latPFC were bilaterally covered by the present probe spatial arrangement. According to the results of the conversion, the arrangement included the latPFC (A3 and C9), the dorsal premotor cortex (PMd; B1, B9, D1 and D9), the dorso-medial part of the sFG, which is adjacent to the pre-SMA region (B7 and D3). The external posterior channels (B3, B5, D5 and D7) were located on the border between the premotor and motor cortices (BA6 and BA4). Specifically, the midpoints of the channels B7 and D3 were located on left and right sFG, whereas the midpoints of the channels A3 and C9 were located on the left and right latPFC, respectively.

fNIRS data analysis

Individual hemodynamic responses were baseline-corrected on a trial-by-trial basis by subtracting the mean intensity of the optical signal recorded during the 2 s preceding trial onset from the overall hemodynamic activity (Schroeter et al., 2002). For each sampling period, artifact rejection thresholds were chosen as the mean response intensity at that timepoint±3 SDs. Trials that contained at least one value exceeding the values of the threshold function were discarded from further analysis.

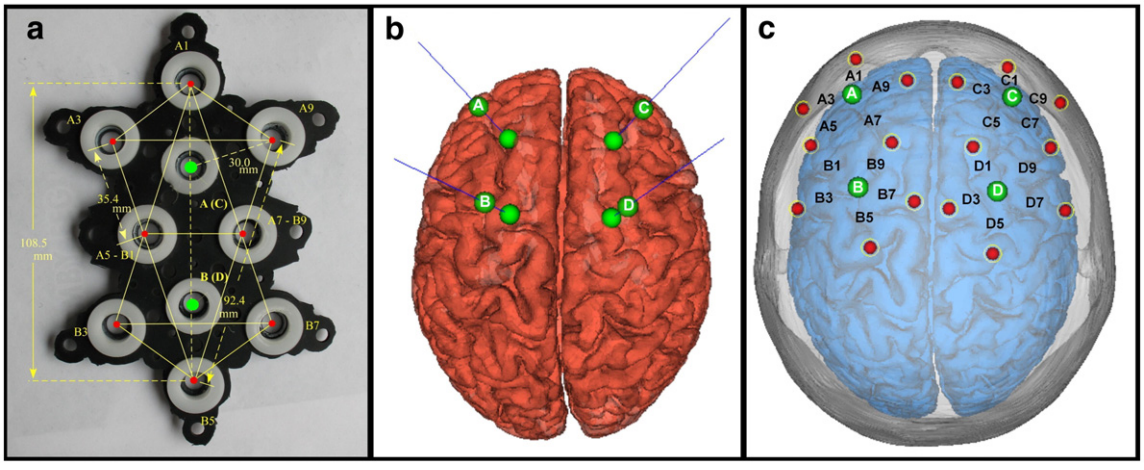

Fig. 2. Probe placement illustration on ICBM 152 template. a) Probe geometry superimposed on the holder. Green circles indicate the position of the detectors. Two holders were placed symmetrically over the left/right hemispheres. b) Top view of brain surface, with the position of detectors on the brain (green dots; A, B, C, D) and their projection on the scalp surface. c) Top view of the scalp surface (opacity 0.6) superimposed on the reference brain surface. The scalp projections of detectors (green dots) and sources (red dots) are based on the geometry of the holder and MNI coordinates approximation of detectors.

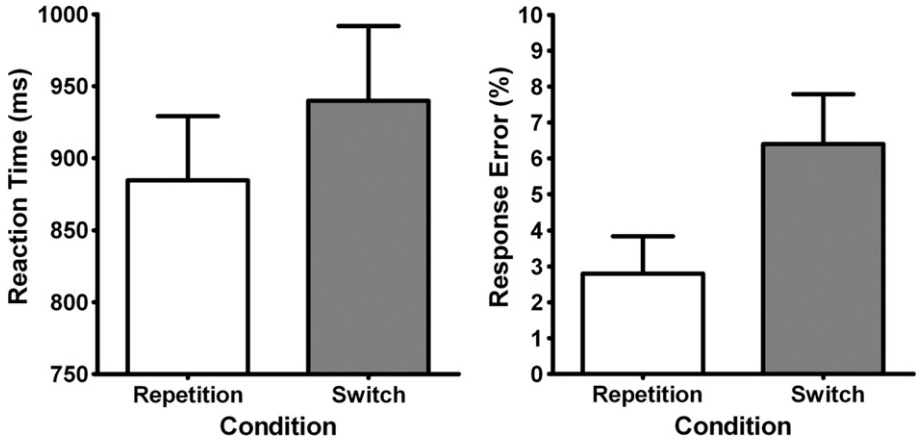

Fig. 3. Behavioral results: Mean RTs (left panel) and mean percentage of errors (right panel). Bars represent standard errors.

Subsequently, the mean ΔHbO and ΔHbR signal intensities during vascular response (3–7 s interval after trial onset) were calculated for each subject and condition. As an estimation of cerebral blood volume, we calculated the concentration of ΔHbT (sum of ΔHbO and ΔHbR; Culver et al., 2005). By repeating the same procedure for each channel, we obtained three individual optical maps (ΔHbO, ΔHbR, and ΔHbT) for switch trials and repetition trials. All the computations were performed using a custom-made code in MatLab (ver. 7.1 SP1).

A random-effect analysis was performed on the data recorded in switch trials using the individual optical maps to identify (via one-tail *t*-tests) the channels showing a significant activation increase relative to the baseline. A second series of one-tail paired *t*-tests was conducted to compare the optical maps of all subjects between switch trials and repetition trials. In these analyses, the false discovery rate method of Benjamini and Hochberg (1995; FDR_{BH}) was employed to correct *p* values based on the proportion of false positives across the active channels (see Genovese et al., 2002, for an application of FDR method in a fMRI study). The value of q specifying the maximum FDR was set to .05, such that no more than an average 5% false positives could be included in the set of significantly active channels for each given statistical test.

The significant *t* values were converted into *z* scores to create *z*-maps as follows. The *z* score of each channel was mapped onto an overlay map (1 mm^3 voxel size) at the correspondent midpoint expressed in MNI coordinates, using the Nifti toolbox (Neuroimaging Informatics Technology Initiative, www.nifti.nimh.nih.gov). A Gaussian blurring filter (SD = 10 mm) was then applied to the overlay map to approximate the area covered by each channel. Finally, the resulting *z*-map was overlaid onto the reference brain using MRicron software (http://www.sph.sc.edu/comd/rorden/mricron/).

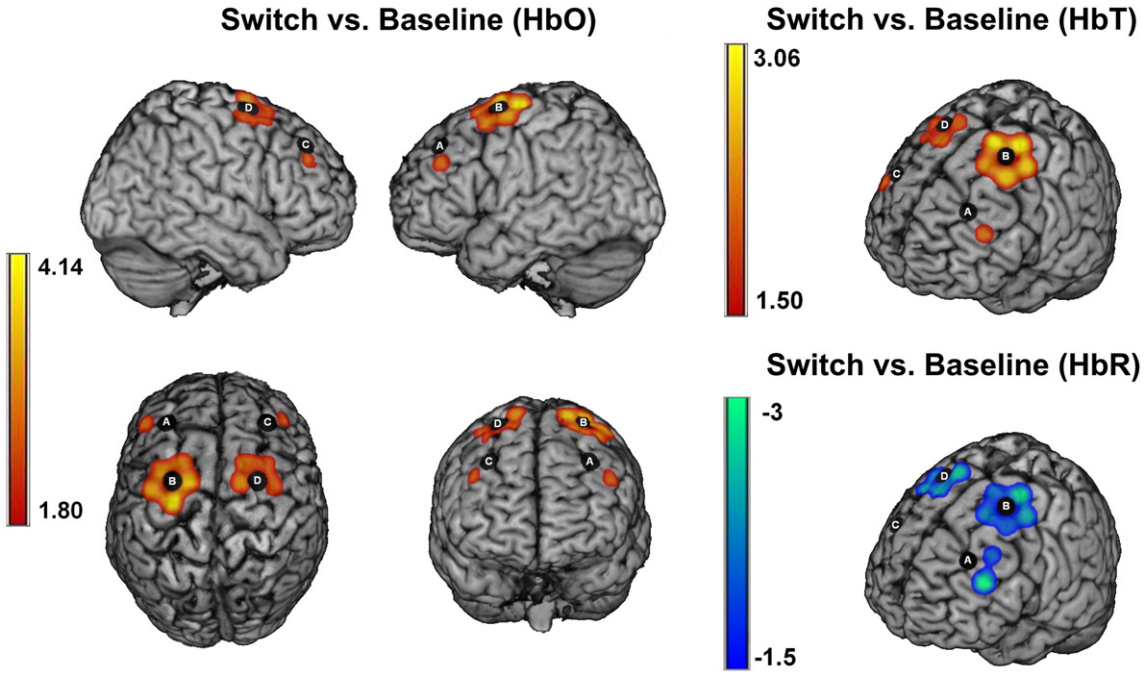

Fig. 4. Statistical (*z*) maps in the switch vs. baseline condition for HbO (left panels), HbT (top right panel), and HbR (bottom right panel). The bilateral activation of premotor areas is evident in all *z*-maps. The HbR concentration map shows a unilateral activation of the latPFC, whereas HbO and HbT concentrations show a bilateral activation of the latPFC (see text for details).

Results

Behavior

A summary of the behavioral results is graphically reproduced in Fig. 3. A one-tail paired *t*-test performed on median RT values considering trial-type (switch vs. repetition) as factor produced a significant result ($t(9)=3.125$, $p<.05$). An analogous *t*-test performed on the percentage of incorrect responses also revealed a significant effect of trial-type ($t(9)=2.53$, $p<.05$). As expected, switch trials were associated with longer RTs and worse accuracy relative to repetition trials.

fNIRS: Repetition/switch versus baseline

A summary of the fNIRS results in the repetition and switch conditions against baseline activation is graphically reproduced in Fig. 4 and in Fig. 5. In the switch vs. baseline condition, illustrated in Fig. 4, the analysis carried out on the *z*-maps revealed positive *z* values for ΔHbO, ΔHbT, and negative *z* values for ΔHbR. Results for the three concentrations were quite consistent. All the *z*-maps showed a broad bilateral activation of the premotor areas, both in the middle frontal gyrus (mFG) and sFG (B1, B7, B9 in the left hemisphere, and D1, D3, and D9 in the right hemisphere), an activation of motor and premotor areas of the left hemisphere (B3 and B5, although a lower activation was found in the correspondent region of the right hemisphere, D7), and a bilateral activation of latPFC (A3 on the left hemisphere and C9 on the right hemisphere, except for HbR that had significant *z* values in the left hemisphere only). Table 1 lists the significantly active channels and the corresponding MNI coordinates and Brodmann areas (BAs). The average *z*-map for ΔHbO, shown in the left panel of Fig. 4, were generated after reducing the FDR-based q to a value of .01 (instead of the standard .05 used in all other cases), due to the enhanced sensitivity of HbO to regional cerebral blood flow (Hoshi et al., 2001; Strangman et al., 2002). Not surprisingly, *z*-maxima for ΔHbO ($z=4.14$, $p<.01$) was found on B5 (i.e., the channel closest to the left motor cortex), likely owing to the use of the right hand for responding. The *z*-minima for

Table 1
Mean concentrations (switch vs. baseline) for all the active channels (*$p<.05$; **$p<.01$)

Ch.	Hb	Mean ± (nM) SD	Statistical Effect (z-value)	MNI Position (x, y, z)	BA	Region
A3	HbO	144.25 ± 132.73	2.68**	−45, 42, 34	BA46	Left latPFC
	HbR	**−33.78 ± 26.08**	**−3.00***			
	HbT	110.48 ± 121.95	2.35**			
A5	HbO	71.14 ± 151.87	n.s.	−41, 28, 46	BA9	Left latPFC
	HbR	−25.18 ± 35.21	−1.96*			
	HbT	91.61 ± 121.52	2.04**			
B1	HbO	186.99 ± 132.39	3.16**	−36, 10, 58	BA6	Left mFG
	HbR	−57.97 ± 81.33	−1.95*			
	HbT	129.03 ± 105.62	2.89**			
B3	HbO	189.55 ± 128.46	3.25**	−43, 3, 60	BA6	Left mFG
	HbR	−50.49 ± 52.56	−2.46*			
	HbT	139.07 ± 112.43	2.91**			
B5	HbO	**275.24 ± 115.30**	**4.14****	−28, −9, 70	BA6	Left sFG
	HbR	−79.97 ± 68.05	−2.82*			
	HbT	**195.27 ± 138.99**	**3.15***			
B7	HbO	239.98 ± 129.36	3.67**	−18, 3, 71	BA6	Left sFG
	HbR	−85.62 ± 112.46	−2.06*			
	HbT	154.36 ± 115.28	3.06*			
B9	HbO	225.08 ± 182.28	2.91**	−22, 15, 64	BA8	Left sFG
	HbR	−61.54 ± 75.69	−2.17*			
	HbT	163.54 ± 159.45	2.57*			
C9	HbO	124.36 ± 109.94	2.75**	40, 45, 32	BA46	Right latPFC
	HbR	−16.17 ± 39.15	n.s.			
	HbT	108.19 ± 106.24	2.56*			
D1	HbO	142.54 ± 124.48	2.77**	18, 15, 64	BA8	Right sFG
	HbR	−33.31 ± 33.99	−2.49*			
	HbT	109.23 ± 116.15	2.42*			
D3	HbO	142.96 ± 109.06	3.02**	16, 2, 70	BA6	Right sFG
	HbR	−69.69 ± 63.88	−2.68*			
	HbT	73.27 ± 90.65	2.16*			
D7	HbO	156.54 ± 153.63	2.56**	39, −1, 62	BA6	Right mFG
	HbR	−39.16 ± 47.77	−2.18*			
	HbT	117.39 ± 143.45	2.18*			
D9	HbO	134.14 ± 132.99	2.54**	34, 14, 58	BA6	Right mFG
	HbR	−31.04 ± 31.88	−2.48*			
	HbT	103.09 ± 136.40	2.05*			

Values in bold represent the *z*-maxima for each concentration.

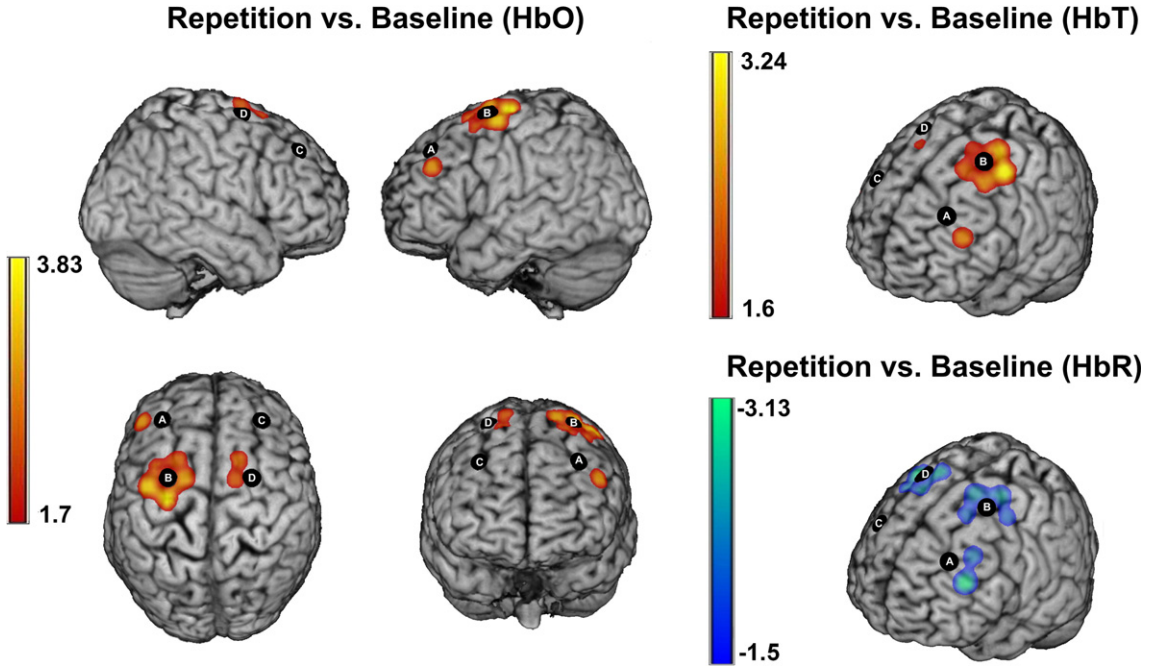

Fig. 5. Statistical (*z*) maps in the repetition vs. baseline condition for HbO (left panels), HbT (top right panel), and HbR (bottom right panel). The bilateral activation of premotor areas is evident in all *z*-maps, with generally weaker activation on the right hemisphere relative to the left hemisphere, and relative also to the activation found in the switch vs. baseline comparison (see Fig. 4).

Table 2
Mean concentration differences (switch minus repetition) for all the active channels (*$p<.05$; ***$p<.001$)

Channel		Mean±SD (nM)	Statistical Effect (z-value)	MNI Position (x, y, z)	BA	Region
B1	HbO	65.16±58.18	2.72*	−36, 10, 58	BA6	Left mFG
B9	HbO	54.24±48.69	2.73*	−22, 15, 64	BA8	Left sFG
B7	HbO	82.65±75.723	2.68*	−18, 3, 71	BA6	Left sFG
	HbT	76.23±49.79	3.31***			

ΔHbR ($z=-3.00$, $p<.05$) was found on the left latPFC. As can be seen in Fig. 4 (bottom right panel), this finding dovetails nicely with the ΔHbR activation of A5 (adjacent to A3). The analysis of ΔHbT was performed considering only channels that the analyses on ΔHbO or ΔHbR values indicated as significantly active. The z-maxima for ΔHbT ($z=3.15$, $p<.05$) was found on B5, consistently with the ΔHbO results. As is evident in Fig. 4 (top right panel), B7 reached also a high z score ($z=3.06$, $p<.05$).

In the repetition vs. baseline condition, illustrated in Fig. 5, the analysis revealed a pattern of activation for all the three concentration indices largely consistent with the pattern evidenced in switch vs. repetition comparison, though characterized by a generally less evident activation of analogous regions in the right hemisphere. Also consistent with the results in the more relevant switch vs. baseline condition was the z-minima found for HbR, following the standard FDR correction, for the left latPFC (−3.13; $p<.05$).

fNIRS: Switch versus repetition

The individual z-maps from the switch and repetition conditions were compared with a paired one-tail t-test carried out on ΔHbO, ΔHbR and ΔHbT data. The t-test on ΔHbR concentration values did not produce any significant result, and was not considered in the following analyses. Table 2 shows the mean hemodynamic HbO and HbT concentrations for the active channels in the vascular response period (3–7 s after trial onset) following the subtraction of the values recorded in repetition trials from the values recorded in switch trials.

The analysis of ΔHbO values indicated a broad activation of the left premotor areas (B1, B7 and B9), including the sFG (B7 and B9), and part of PMd in the mFG (B1). The z scores of B1, B7 and B9 were similar (2.72, 2.68 and 2.72, respectively, $p<.05$), indicating a coarse increase in HbO concentration over BA6. The analysis of HbT values, which are known to provide brain activation maps with better spatial resolution than the other indices of concentration (Culver et al., 2005), revealed a significant activation of the most medial part of the sFG (B7; $z=3.31$, $p<.01$). Fig. 6 shows the pattern of activation found in the present study (leftmost panel: HbT; central panel: HbO), compared with the pattern of activation reported by Crone et al. (2006; rightmost panel).

fNIRS: LatPFC versus sFG

To provide a statistical test of the functional dissociation between latPFC and sFG areas, an analysis of variance (ANOVA) was conducted on the ΔHbT values that considered trial-type (switch vs. repetition) as a within-subject factor, and region (A3: left latPFC vs. B7: left sFG) as a between-subject factor. We deemed appropriate to restrict our analysis on values recorded from the left latPFC, based on prior results suggesting a more substantial involvement of this region (relative to the homologous region in the right hemisphere) in stimulus–response mapping rule representation (Bunge et al., 2003; Crone et al., 2006).

A summary of the results is reported in Fig. 7. The ANOVA revealed a significant effect of trial-type ($F(1, 18)=11.5$, $p<.001$) and, importantly, a significant interaction between trial-type and region ($F(1, 18)=4.8$, $p<.05$). The results of a one-tail t-test indicated that sFG activity was strongly modulated in switch trials relative to repetition trials (154.36±115.28 nM and 78.13±136.90 nM, respectively, $t(1, 9)=4.84$, $p<.001$), whereas the activity in the left latPFC in switch trials and repetition trials was not significantly different (110.47±121.95 nM and 93.93±105.67 nM, respectively, $t(1, 9)=0.74$, $p=.478$). An equivalent analysis was performed on ΔHbO concentration values. The three ΔHbO active channels (B1, B7, and B9) were separately compared with the left latPFC channel (A3), using the same ANOVA's design adopted for ΔHbT analysis. A significant effect of trial-type was found for each channel (B1: $F(1, 18)=8.42$, $p<.01$; B7: $F(1, 18)=9.67$, $p<.01$; B9: $F(1, 18)=7.297$, $p<.05$). However, a marginally significant interaction between trial-type and region was found only for B7 ($F(1, 18)=3.52$, $p=.077$), a result that was generally consistent with the results observed in the analysis of HbT values.

In order to provide a direct quantification of switch-related modulations of activity in the latPFC and sFG areas, effect sizes (d) were calculated following the algorithm adopted by Cohen

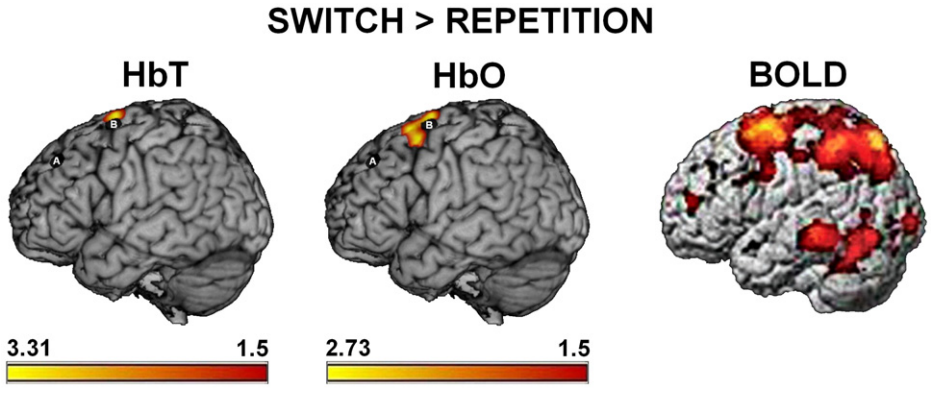

Fig. 6. Statistical (z) maps in the switch-minus-repetition condition (leftmost panel: HbT; central panel: HbO), which can be compared with the pattern of activation reported by Crone et al. (2006; rightmost panel).

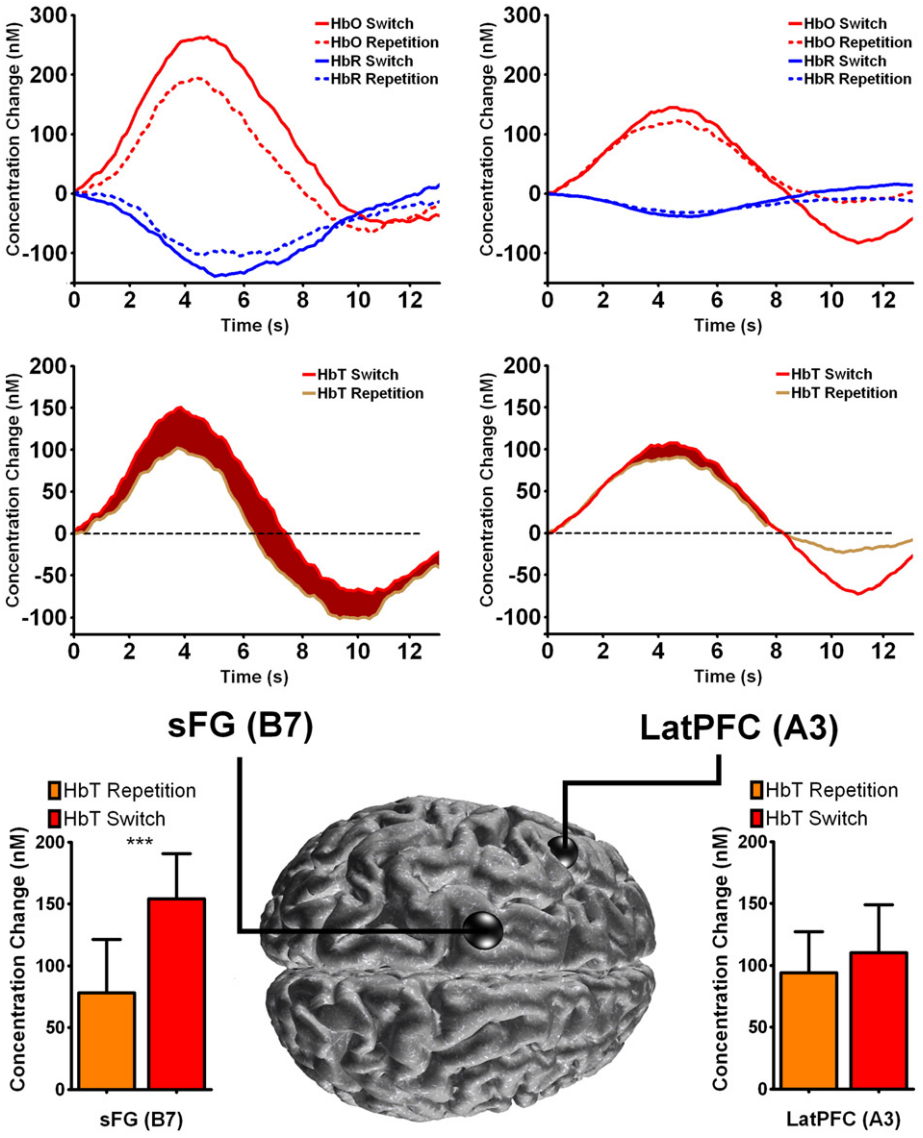

Fig. 7. Top: Temporal functions averaged over all subjects (time-course) of the hemodynamic response (top: HbO and HbR; bottom: HbT) for sFG (left) and latPFC (right) areas in switch trials and repetition trials. Time 0 corresponds to the trial onset. For display purposes, the mean concentration recorded for all indices in the interval starting 1 s pre-stimulus and ending 1 s post-stimulus onset was set to 0 nM, as in Schroeter et al. (2007). Bottom: Bar charts illustrating the mean hemodynamic concentration changes of HbT. The sFG (left side) corresponds to channel B7 and the latPFC corresponds to channel A3 (right side). The black circular regions correspond to the midpoints of B7 and A3 channels once mapped onto the reference brain (*** $p<.001$).

(1988) and Schroeter et al. (2003), who proposed to derive d as the difference between the mean d values in switch trials (m_S) and the mean d values in repetition trials (m_R), divided by the standard deviation of d values in repetition trials (SD_R). The mean effect size for sFG ($d=0.98\pm0.64$) was larger than the effect size for latPFC ($d=0.16\pm0.67$).

Discussion

The primary scope of the present investigation was to test a specific hypothesis, proposed by Crone et al. (2006), about the different role played by two specific cortical areas, namely, the latPFC and the sFG, in the complex operations required to flexibly coordinate the execution of two different tasks in the task-switching paradigm. This hypothesis, which was developed on the basis of fMRI evidence, ascribes to the latPFC a set of mental subroutines including loading, maintaining and retrieving distinct stimulus–response mapping rules for the correct performance in the task-switching paradigm. This hypothesis, in addition, posits that regions in the sFG, such as the pre-SMA and SMA areas, would instead be responsible of alternating between distinct stimulus-response mapping rules, as is forcibly required in switch trials. To test this hypothesis, we employed a variant of the task-switching paradigm implementing a pair of tasks that were carefully balanced along several critical dimensions. The stimuli used in the present context (the symbols '+' and '−') were selected so as to impose minimal demands on the perceptual side. Each of these stimuli was associated with a speeded two-alternative choice task and, crucially, the set of possible responses across the tasks was the same (the keys 'M' and 'N'). In this regard, the stimulus–response mapping rules in the two tasks were bivalent, and identical with respect to the load imposed by each stimulus–response mapping rule on working memory. The color of the stimuli (red or green) served as the cue for the adoption of one or the other stimulus–response mapping rule,

and this expedient was adopted in order to minimize the potential impact of anticipatory bias in performing the present task-switching design. Finally, and importantly, switch trials and repetition trials were randomly organized in the uninterrupted sequence of trials subjects had to perform, and equally likely to occur during the sequence.

The results were clear-cut, both behaviorally and neuroanatomically. Behaviorally, as was expected with the use of bivalent rules, the analysis of RTs and accuracy indicated a pronounced switch cost, with longer RTs and worse accuracy in switch trials relative to repetition trials. The fNIRS results showed that both the latPFC and sFG were actively engaged during the execution of our task-switching paradigm. As is evident in Figs. 4 and 5, the fNIRS results indicated a significant bilateral activation of the latPFC and of the m/sFG. In particular, in line with prior neuroimaging investigations, the *z*-minima for ΔHbR were recorded in the left latPFC, and left sFG reached high *z*-scores both for ΔHbO and ΔHbT concentrations. In this regard, the fNIRS results corroborate the corollary of Crone's et al. (2006) hypothesis that predicts the involvement of both the latPFC and the sFG in the flow of processing subtended in task-switching (see also Dreher and Grafman, 2003; Rushworth et al., 2002, for converging evidence).

Based on the assumption that switch trials and repetition trials in the present paradigm did not differ for factors other than those implicated in switching between stimulus–response mapping rules, we subtracted, for all concentration indices, the overall level of cortical activation in repetition trials from the cortical activation in switch trials in the attempt to isolate the neural locus of task-set reconfiguration. The HbT results were of particular interest following subtraction, since HbT is thought to provide brain activation maps with enhanced spatial resolution relative to the other concentration indices (Culver et al., 2005). Interestingly, the remaining significant activity following subtraction was entirely confined to the sFG (the area labeled B7), and this is all the most relevant based on the particularly conservative correction criterion applied in order to obtain this result (i.e., when a single channel is significantly active, the FDR_{BH} correction amounts to a Bonferroni correction; Singh and Dan, 2006). More specifically, the analysis of the effect size of the switch-minus-repetition modulation revealed the specific involvement of the left sFG in switching between stimulus–response mapping rules ($d=0.94$). This second set of results further supports Crone's et al. (2006) hypothesis that the sFG is the primary brain locus implementing the set of functional operations subtended in switching between stimulus–response mapping rules, or, more traditionally, in task-set reconfiguration operations. As further support of Crone's et al. (2006), and of some of the studies briefly reviewed in the Introduction (e.g., Dove et al., 2000; Dreher and Grafman, 2003; Dreher et al., 2002), it must be noted that the position of B7 in present investigation overlapped to a large extent with the region in MNI coordinates (−12, 8, 60; left sFG) in which the *z*-maxima was found by Crone et al. (2006) when comparing switch trials and repetition trials. It must be underlined that the present conclusions are conceptually limited to task-switching paradigms employing centrally displayed stimuli associated with bivalent stimulus–response rules. Indeed, prior studies on the neural basis of response selection and WM maintenance of spatially distributed stimuli have pointed to the selective involvement of dorsal regions of the PFC, in addition to the presently documented involvement of the latPFC, in the maintenance of stimulus–response rules (e.g., Rowe et al., 2000; Schumacher et al., 2007).

A number of considerations are in order concerning prior studies reporting results which are not entirely congruent with the results of the present investigations. In particular, we focus in the forthcoming paragraphs on studies suggesting a link between the activation of the latPFC and the alternation between distinct stimulus–response mapping rules, or task-set reconfiguration. The following considerations move from the assumption, which we reiterate, that stimuli and responses in the present paradigm were identical in the two alternating tasks, which, for these reasons, were hypothesized to impose an identical maintenance load on working memory. Furthermore, given that the stimulus feature cuing subjects for the adoption of either task-set was the color of the stimuli, which was varied unpredictably to subjects and changed with identical frequency, we further assumed that anticipatory and/or preparation biases in the present design were reduced to a minimum. Each of these methodological constraints may have been crucial to determine the specific pattern of results obtained in this context.

In a subset of previous task-switching studies, one suspect is that switching between tasks was confounded with a bias in preparatory state. A factor that may influence preparatory states is task-order predictability. To note, when task order is predictable, subjects tend to adopt different strategies (Gopher et al., 2000; Strayer and Kramer, 1994), and modulate their preparatory state based on information about task order. Such information has been shown to be effective in reducing RTs in both switch and repetition trials (Sohn and Carlson, 2000). Interestingly, using a task order that was predictable, Dreher et al. (2002) reported a general activation state of the latPFC, that was interpreted as a reflection of preparatory state variations that were not, however, specifically related to task-set reconfiguration.

Dove et al. (2000) found an enhanced activation of a network of brain regions (including latPFC and sFG) in switch trials relative to repetition trials. As the authors explicitly acknowledged, the frequency of switch trials in their design was much reduced relative to repetition trials, and this may have induced a sort of odd-ball effect (upon the occurrence of a switch trials) that was not separable from switch costs.

Cueing has also been shown to induce effects in task-switching that can hardly be taken as selectively associated with task-set reconfiguration. Barch et al. (1997) have described a protracted activation of the latPFC, that overlapped temporally with the period of time during which a prestimulus was maintained in working memory. Incidentally, Brass and von Cramon (2002) have shown that cuing modulates activity in the anterior portion of the sFG. Activity in the latPFC is notoriously correlated with working memory load (e.g., Cohen et al., 1997; Manoach et al., 1997; and Curtis and D'Esposito, 2003, for a review), and this may explain why, in task-switching paradigms that used univalent stimulus–response mapping rules (i.e., categorically distinct stimuli between tasks associated with distinct response sets), variations in latPFC activity were observed when subjects switched between task-sets (Crone et al., 2006). In these circumstances, it is likely that variations in latPFC activity reflected changes in working memory load (i.e., the need to actively retrieve and/or select a relevant rule) rather than an involvement in task-set reconfiguration. Importantly, this consideration is congruent with the results of prior studies examining the role of latPFC in

learning by trial and error arbitrary visuo-motor associations (e.g., distinct visual patterns to be mapped to distinct motor responses; Murray et al., 2000; Toni and Passingham, 1999; Toni et al., 2001), and more abstract sets of rules (Brass and von Cramon, 2002; Bunge et al., 2003).

One possible criticism to the present work is related to narrowing the present set of regions of interest to just the latPFC and the sFG. In fact, the results of two studies suggest that other regions, that we could not monitor due to the structural constraints imposed by the optical device employed in the present investigation, may be involved in task-switching, such as the anterior cingulate cortex (ACC; Dove et al., 2000), and the parietal cortex (Kimberg et al., 2000; Sohn et al., 2000). The coverage of a larger portion of brain tissue using fNIRS is something that we are currently pursuing in our laboratory and, at present, we cannot exclude the possibility that part of the activation of the left sFG on switch trials resulted from the contribution of activation in superior regions of the ACC projecting to regions closer to the cortical surface, in light of the somatotopic organization of the caudal portion of the ACC and the production of responses in our paradigm through the use of the right hand (e.g., Barch et al., 2001). It may be nonetheless worth mentioning that ACC has been hypothesized to be more likely involved in the resolution of response conflicts, as suggested by the results of the dual-task study of Dreher and Grafman (2003), rather than in task-set reconfiguration per se. The ACC involvement in task switching is therefore likely to be epiphenomenal to the need of monitoring performance for avoiding incorrect responses when a particular stimulus–response mapping rule is already influencing the flow of processing required for the execution of a particular task (e.g., Rushworth et al., 2004).

Furthermore, the technical limitations raised above did not allow us to inspect additional cortical areas which have been hypothesized to play a role in the coordination of complex high-level cognitive activities. One of such areas is the parietal cortex. Regions in the surroundings of the intra-parietal sulcus (IPS), for instance, have been shown to be contribute massively to the processing and maintenance of task-relevant information (Wojciulik and Kanwisher, 1999), being the primary node for re-entrant activation originating in the dorso-lateral regions of the PFC (Dreher and Grafman, 2003) under conditions in which, as in the present study, the imperative stimuli are displayed through the visual modality (e.g., Dell'Acqua et al., 2006a,b; Klaver et al., 1999). However, as argued by Dreher and Grafman on the basis of a direct comparison between dual-task and task-switch conditions, neither the dorsal parietal cortex nor the IPS appear to be determinant in task-alternation, though we recognize that a promising avenue for future research may be to extend the coverage for the detection of optical signal modulations also to these areas, in order to better understand their functional role using a design that, as the present, allowed us to carefully control for factors other than those implicated in the reconfiguration of task-sets.

References

Allport, A., Styles, E.A., Hsieh, S., 1994. Shifting intentional set: exploring the dynamic control of tasks. In: Umiltà, C., Moscovitch, M. (Eds.), Attention and performance XV: Conscious and nonconscious information processing. MIT Press, Cambridge, MA, pp. 421–452.

Arbuthnott, K., Frank, J., 2000. Executive control in set switching: residual switch cost and task-set inhibition. Can. J. Exp. Psychol. 54, 33–41.

Ayaz, H., Izzetoglu, M., Platek, S.M., Bunce, S., Izzetoglu, K., Pourrezaei, K., Onaral, B., 2006. Registering fNIR data to brain surface image using MRI templates. Proceedings of the 28th IEEE EMBS Annual International Conference New York City, USA.

Baddeley, A., Emslie, H., Kolodny, J., Duncan, J., 1998. Random generation and the executive control of working memory. Q. J. Exp. Psychol., A 51, 819–852.

Barch, D.M., Braver, T.S., Nystrom, L.E., Forman, S.D., Noll, D.C., Cohen, J.D., 1997. Dissociating working memory from task difficulty in human prefrontal cortex. Neuropsychologia 35, 1373–1380.

Barch, D.M., Braver, T.S., Akbudak, E., Conturo, T., Ollinger, J., Snyder, A., 2001. Anterior cingulate cortex and response conflict: effects of response modality and processing domain. Cereb. Cortex 11, 837–848.

Benjamini, Y., Hochberg, Y., 1995. Controlling the false discovery rate: a practical and powerful approach to multiple testing. J. R. Statist. SocSer. B, 57, 289–300.

Brass, M., von Cramon, D.Y., 2002. The role of the frontal cortex in task preparation. Cereb. Cortex 12, 908–914.

Brett, M., Christoff, K., Cusack, R., Lancaster, J., 2001. Using the Talairach atlas with the MNI template. NeuroImage 13, S85.

Bunge, S.A., Kahn, I., Wallis, J.D., Miller, E.K., Wagner, A.D., 2003. Neural circuits subserving the retrieval and maintenance of abstract rules. J. Neurophysiol. 90, 3419–3428.

Cohen, J., 1988. Statistical Power Analysis for the Behavioral Sciences, 2nd ed. Lawrence Earlbaum Associates, Hillsdale, NJ.

Cohen, J.D., Perlstein, W.M., Braver, T.S., Nystrom, L.E., Noll, D.C., Jonides, J., Smith, E.E., 1997. Temporal dynamics of brain activation during a working memory task. Nature 386, 604–607.

Cope, M., Delpy, D.T., 1988. System for long-term measurement of cerebral blood and tissue oxygenation on newborn infants by near infra-red transillumination. Med. Biol. Eng. Comput. 26, 289–294.

Crone, E.A., Wendelken, C., Donohue, S.E., Bunge, S.A., 2006. Neural evidence for dissociable components of task-switching. Cereb. Cortex 16, 475–486.

Culver, J.P., Siegel, A.M., Franceschini, M.A., Mandeville, J.B., Boas, D.A., 2005. Evidence that cerebral blood volume can provide brain activation maps with better spatial resolution than deoxyhemoglobin. NeuroImage 27, 947–959.

Curtis, C.E., D'Esposito, M., 2003. Persistent activity in the prefrontal cortex during working memory. Trends Cogn. Sci. 7, 415–423.

Dell'Acqua, R., Pashler, H., Stablum, F., 2003. Multi-tasking costs in closed-head injury patients: A fine-grained analysis. Exp. Brain Res. 152, 29–41.

Dell'Acqua, R., Sessa, P., Jolicœur, P., Robitaille, N., 2006a. Spatial attention freezes during the attentional blink. Psychophysiology 43, 394–400.

Dell'Acqua, R., Sessa, P., Pashler, H., 2006b. An assessment of dual-task costs in closed-head injury patients using Cohen's effect size estimation method. Psychol. Res. 70, 553–561.

Dove, A., Pollmann, S., Schubert, T., Wiggins, C.J., von Cramon, D.Y., 2000. Prefrontal cortex activation in task switching: an event-related fMRI study. Cogn. Brain Res. 9, 103–109.

Dreher, J., Berman, K., 2002. Fractionating the neural substrate of cognitive control processes. Proc. Natl. Acad. Sci. U. S. A. 99, 14595–14600.

Dreher, J.C., Grafman, J., 2003. Dissociating the roles of the rostral anterior cingulate and the lateral prefrontal cortices in performing two tasks simultaneously or successively. Cereb. Cortex 13, 329–339.

Dreher, J.C., Koechlin, E., Ali, S.O., Grafman, J., 2002. The roles of timing and task order during task switching. NeuroImage 17, 95–109.

Duncan, A., Meek, J.H., Clemence, M., Elwell, C.E., Fallon, P., Tyszczuk, L., Cope, M., Delpy, D.T., 1996. Measurement of cranial optical path length as a function of age using phase resolved near infrared spectroscopy. Pediatr. Res. 39, 889–894.

Franceschini, M.A., Toronov, V., Filiaci, M.E., Gratton, E., Fantini, S., 2000. On-line optical imaging of the human brain with 160-ms temporal resolution. Opt. Express 6, 49–57.

Genovese, C.R., Lazar, N.A., Nichols, T., 2002. Thresholding of statistical maps in functional neuroimaging using the false discovery rate. NeuroImage 15, 870–878.

Gopher, D., Armony, L., Greenshpan, Y., 2000. Switching tasks and attention policies. J. Exp. Psychol. Gen. 129, 308–339.

Hoshi, Y., Kobayashi, N., Tamura, M., 2001. Interpretation of near-infrared spectroscopy signals: a study with a newly developed perfused rat brain model. J. Appl. Physiol. 90, 1657–1662.

Hoshi, Y., Tsou, B.H., Billock, V.A., Tanosaki, M., Iguchi, Y., Shimada, M., Shinba, T., Yamada, Y., Oda, I., 2003. Spatiotemporal characteristics of hemodynamic changes in the human lateral prefrontal cortex during working memory tasks. NeuroImage 20, 1493–1504.

Jersild, A.T., 1927. Mental set and shift. Arch. Psychol. 89 whole number.

Kimberg, D.Y., Aguirre, G.K., D'Esposito, M., 2000. Modulation of task-related neural activity in task-switching: an fMRI study. Cogn. Brain Res. 10, 189–196.

Klaver, P., Talsma, D., Wijers, A.A., Heinze, H.-J., Mulder, G., 1999. An event-related brain potential correlate of visual short-term memory. NeuroReport 10, 2001–2005.

Manoach, D.S., Schlaug, G., Bettina, S., Darby, D.G., Bly, B.M., Benfield, A., Edelman, R.R., Warach, S., 1997. Prefrontal cortex fMRI signal changes are correlated with working memory load. NeuroReport 8, 545–549.

Mayr, U., Keele, S.W., 2000. Changing internal constraints on action: the role of backward inhibition. J. Exp. Psychol. Gen. 129, 4–26.

Mecklinger, A.D., von Cramon, D.Y., Springer, A., Matthes-von Cramon, G., 1999. Executive control functions in task switching: evidence from brain injured patients. J. Clin. Exp. Neuropsychol. 21, 606–619.

Meiran, N., 1996. Reconfiguration of processing mode prior to task performance. J. Exper. Psychol., Learn., Mem., Cogn. 22, 1423–1442.

Meiran, N., Chorev, Z., Sapir, A., 2000. Component processes in task switching. Cogn. Psychol. 41, 211–253.

Miyai, I., Tanabe, H.C., Sase, I., Eda, H., Oda, I., Konishi, I., Tsunazawa, Y., Suzuki, T., Yanagida, T., Kubota, K., 2001. Cortical mapping of gait in humans: a near-infrared spectroscopic topography study. NeuroImage 14, 1186–1192.

Monsell, S., 2003. Task switching. Trends Cogn. Sci. 7, 134–140.
Murray, E.A., Bussey, T.J., Wise, S.P., 2000. Role of prefrontal cortex in a network for arbitrary visuomotor mapping. Exp. Brain Res. 133, 114–129.
Okamoto, M., Dan, I., 2005. Automated cortical projection of head-surface locations for transcranial functional brain mapping. NeuroImage 26, 18–28.
Okamoto, M., Dan, H., Sakamoto, K., Takeo, K., Shimizu, K., Kohno, S., Oda, I., Isobe, S., Suzuki, T., Kohyama, K., Dan, I., 2004. Three-dimensional probabilistic anatomical cranio-cerebral correlation via the international 10–20 system oriented for transcranial functional brain mapping. NeuroImage 21, 99–111.
Rogers, R.D., Monsell, S., 1995. Costs of a predictable switch between simple cognitive tasks. J. Exp. Psychol. Gen. 124, 207–231.
Rogers, R.D., Sahakian, B.J., Hodges, J.R., Polkey, C.E., Kennard, C., Robbins, T.W., 1998. Dissociating executive mechanisms of task control following frontal lobe damage and Parkinson's disease. Brain 121, 815–842.
Rowe, J.B., Toni, I., Josephs, O., Frackowiak, R.S.J., Passingham, R.E., 2000. The prefrontal cortex: response selection or maintenance in working memory? Science 288, 1656–1660.
Rubinstein, J.S., Meyer, D.E., Evans, J.E., 2001. Executive control of cognitive processes in task switching. J. Exp. Psychol. Gen. Hum. Percept. Perform. 27, 763–797.
Rushworth, M.F.S., Hadland, K.A., Paus, T., Sipila, P.K., 2002. Role of the human medial frontal cortex in task switching: a combined fMRI and TMS study. J. Neurophysiol. 87, 2577–2592.
Rushworth, M.F.S., Walton, M.E., Kennerley, S.W., Bannerman, D.M., 2004. Action sets and decisions in the medial frontal cortex. Trends Cogn. Sci. 8, 410–417.
Sato, H., Takeuchi, T., Sakai, K.L., 1999. Temporal cortex activation during speech recognition: an optical topography study. Cognition 73, B55–B66.
Schroeter, M.L., Zysset, S., Kupka, T., Kruggel, F., Cramon, D.Y., 2002. Near-infrared spectroscopy can detect brain activity during a color-word matching Stroop task in an event-related design. Hum. Brain Mapp. 17, 61–71.
Schroeter, M.L., Zysset, S., Kruggel, F., von Cramon, D.Y., 2003. Age-dependency of the hemodynamic response as measured by functional near-infrared spectroscopy. NeuroImage 19, 555–564.
Schroeter, M.L., Bucheler, M.M., Muller, K., Uludag, K., Obrig, H., Lohmann, G., Tittgemeyer, M., Villringer, A., Cramon, D.Y., 2004. Towards a standard analysis for functional near-infrared imaging. NeuroImage 21, 283–290.
Schroeter, M.L., Cutini, S., Wahl, M.M., Scheid, R., von Cramon, D.Y., 2007. Neurovascular coupling is impaired in cerebral microangiopathy: an event-related Stroop study. NeuroImage 34, 26–34.
Schumacher, E.H., Cole, M.W., D'Esposito, M., 2007. Selection and maintenance of stimulus-response rules during preparation and performance of a spatial choice-reaction task. Brain Res. 1136, 77–87.
Sevick, E.M., Chance, B., Leigh, J., Nioka, S., Maris, M., 1991. Quantitation of time- and frequency-resolved optical spectra for the determination of tissue oxygenation. Anal. Biochem. 195, 330–351.
Shimada, S., Hiraki, K., Matsuda, G., Oda, I., 2004. Decrease in prefrontal hemoglobin oxygenation during reaching tasks with delayed visual feedback: a near-infrared spectroscopy study. Cogn. Brain Res. 20, 480–490.
Singh, A., Dan, I., 2006. Exploring the false discovery rate in multichannel NIRS. NeuroImage 33, 542–549.
Singh, A., Okamoto, M., Dan, H., Jurcak, V., Dan, I., 2005. Spatial registration of multi-channel multi-subject fNIRS data to MNI space without MRI. NeuroImage 27, 842–851.
Slagter, H.A., Weissman, D.H., Giesbrecht, B., Kenemans, J.L., Mangun, G.R., Kok, A., Woldorff, M.G., 2006. Brain regions activated by endogenous preparatory set-shifting as revealed by fMRI. Cogn. Aff. Behav. Neuros. 6, 175–189.
Sohn, M.H., Carlson, R.A., 2000. Effects of repetition and foreknowledge in task-set reconfiguration. J. Exp. Psychol. Learn. Mem. Cogn. 26, 1445–1460.
Sohn, M.H., Ursu, S., Anderson, J.R., Stenger, V.A., Carter, C.S., 2000. The role of prefrontal cortex and posterior parietal cortex in task switching. Proc. Natl. Acad. Sci. U. S. A. 97, 13448–13453.
Strangman, G., Boas, D.A., Sutton, J.P., 2002. Non-invasive neuroimaging using near-infrared light. Biol. Psychiatry 52, 679–693.
Strayer, D.L., Kramer, A.F., 1994. Strategies and automaticity: I. Basic findings and conceptual framework. J. Exp. Psychol. Learn. Mem. Cogn. 20, 318–341.
Stuss, D.T., Levine, B., Alexander, M.P., Hong, J., Palumbo, C., Hamer, L., Murphy, K.J., Izukawa, D., 2000. Wisconsin Card Sorting test performance in patients with focal frontal and posterior brain damage: effects of lesion location and test structure on separable cognitive processes. Neuropsychologia 38, 388–402.
Taga, G., Asakawa, K., Maki, A., Konishi, Y., Koizumi, H., 2003. Brain imaging in awake infants by near-infrared optical topography. Proc. Natl. Acad. Sci. U. S. A. 100, 10722–10727.
Tanosaki, M., Hoshi, Y., Iguchi, Y., Oikawa, Y., Oda, I., Oda, M., 2001. Variation of temporal characteristics in human cerebral hemodynamic responses to electric median nerve stimulation: a near-infrared spectroscopic study. Neurosci. Lett. 316, 75–78.
Toni, I., Passingham, R.E., 1999. Prefrontal-basal ganglia pathways are involved in the learning of arbitrary visuomotor associations: a PET study. Exp. Brain Res. 127, 19–32.
Toni, I., Ramnani, N., Josephs, O., Ashburner, J., Passingham, R.E., 2001. Learning arbitrary visuomotor associations: temporal dynamic of brain activity. NeuroImage 14, 1048–1057.
Villringer, A., Chance, B., 1997. Non-invasive optical spectroscopy and imaging of human brain function. Trends Neurosci. 20, 435–442.
Waszak, F., Hommel, B., Allport, A., 2003. Task-switching and long-term priming: role of episodic S-R bindings in task-switch costs. Cogn. Psychol. 46, 361–413.
Wojciulik, E., Kanwisher, N., 1999. The generality of parietal involvement in visual attention. Neuron 23, 747–764.
Yeung, N., Monsell, S., 2003. Switching between tasks of unequal familiarity: the role of stimulus-attribute and response-set selection. J. Exp. Psychol. Gen. Hum. Percept. Perform. 29, 455–469.